# Influence of confinement dependent failure processes on rock mass strength at depth

Benoît Valley, Bo-Hyun Kim, Fidelis T. Suorineni, Navid Bahrani & Rob P. Bewick
*MIRARCO/Geomechanics Research Center, Sudbury, Canada*

Peter K. Kaiser
*CEMI – Center for Excellence in Mining Innovation, Sudbury, Canada*

**ABSTRACT:** Changes of failure mechanism with increasing confinement, from tensile to shear dominated failure, is widely observed in the rupture of samples in laboratory and in rock masses in situ. However, common failure criteria typically consider only shear mechanisms. A hybrid criteria based on a sigmoid function is introduced to account for a transition from tensile to shear dominated failure with increasing confinement. When evaluated by fitting to an extensive laboratory database the sigmoid criteria does not provide a better fit compared to the Hoek-Brown failure envelope, but provides insight into rock strength controlling factors that have significant consequences with respect to the interpretation of laboratory test results. It also leads to a differentiated approach for design by considering two types of behaviour process: 1) in the inner shell, i.e. the direct vicinity of openings, the failure mode is dominated by tensile cracking leading to spalling and related geometric dilation processes and 2) in the outer shell, i.e. remote from excavations, where confinement promotes interlock, we suggest that rock masses could be significantly stronger than predicted by standard approaches.

**SUBJECT:** Site investigation and field observations

**KEYWORDS:** site characterization, rock properties

## 1 INTRODUCTION

An increasing number of mining and civil tunneling projects are being developed at great depth (>2 km). At these depths, in situ stresses exceed the confinement levels that are: (a) typically applied in standard laboratory tests; and (b) for which empirical approaches for rock mass strength evaluation are calibrated. Thus, such empirical relations can be misleading when designing underground infrastructures at great depth, potentially resulting in costly mistakes. Designing at depth, outside the calibration range of empirical methods, may result in over conservative or inadequate designs by not properly anticipating the behavior of the rock mass.

The first part of this paper presents results which illustrate the effect of confinement dependent changes in failure mechanism on the failure envelope for intact rock. At low confinement, tensile mechanisms dominate rock failure. The reasons for this, even in an overall compressive stress field, have been explained by the stress pattern at the tip of elliptical flaws (e.g. Griffith, 1920; Gramberg, 1989) and the presence of heterogeneities (Diederichs, 1994; Valley et al., 2010 ; Lan et al., 2010). With increasing confinement, unstable tensile crack propagation is inhibited resulting in the formation of shear bands and the overall failure of the sample through shear processes.

As flaws and heterogeneities are also part of rock masses, one should expect that similar changes of failure mechanisms occur as the confinement on rock masses increases. As current empirical approaches (e.g. the Geological Strength Index, *GSI* and the generalized Hoek-Brown failure criterion) to estimate the rock mass strength are solely calibrated on low confinement data (failure of excavation walls), such approaches will not embed the change of failure mechanism from tensile dominated at low confinement to shear dominated at high confinement. The hypothesized consequence of this is an underestimation of rock mass strength under confinement (e.g. for pillar design) and the lack of anticipation of the potential rock mass behavior at depth (e.g. yielding ground vs. bursting ground). The second part of this paper reports findings from on-going research on this topic, suggesting practical approaches for consideration in mine design at depth.

## 2 FAILURE OF INTACT ROCK

### 2.1 *The consideration of failure process change with increasing confinement*

The observation of the failure mode of laboratory samples under uniaxial loading ($\sigma_3$=0) clearly highlights the importance of tensile mechanisms (e.g. Gramberg, 1989). Often, the failure of the sample is entirely due to through going axial fractures on which fractographic patterns clearly point toward the tensile mode (mode I). Such mechanisms, often referred to as axial splitting, is common for most rock types and is particularly developed in hard rocks, homogeneous fine-grained rocks and medium to coarse grained crystalline rocks. Generally these rocks are referred to as brittle rocks and their failure as brittle failure. The term brittle has multiple uses in rock mechanics and geology. In this paper it will be used as a descriptor of rocks with failure dominated by tensile damage initiation and propagation in the pre-peak domain.

When confinement is increased, tensile crack propagation is progressively inhibited (Hoek and Bieniawski, 1965, their Fig. 6). Tensile mechanisms are present in samples failing under confinement, but unstable crack propagation resulting in axial splitting is prevented. At peak strength, the failure is usually controlled by the coalescence of micro-cracks forming a macroscopic shear band (Kemeny and Cook, 1987).

While observational evidence in the change in failure mechanism is common in the literature, the interpretation of test results in terms of failure criteria is not consistent with this transition. The two most common criteria used in rock mechanics, Mohr-Coulomb and Hoek-Brown, are monotonic linear or steadily curved, implying that a single mechanism contributes to the rock ultimate strength.

Based on the assumption that the change of failure mechanism with confinement should be reflected in the failure envelope, Kaiser and Kim (2008), fitted laboratory testing data with a sigmoid function enabling a transition from lower strength at low confinement to higher strength at high confinement. An example of fit using a sigmoid function is presented on Fig. 1 (blue curve). This failure envelope is parameterized with the common Uniaxial Compressive Strength (*UCS*, called $UCS_I$ in Kaiser and Kim, 2008) and the Apparent Compressive Strength (*ACS*, Steiner et al., 2010, called $UCS_{II}$ in Kaiser and Kim, 2008). Further parameters describe the overall slope of the failure envelope and the shape of the transition (see Kaiser & Kim, 2008 and Kim & Kaiser, 2009 for details).

The transition typically occurs at confinement levels smaller than about 1/10 of *UCS*. This is justified by the fact that tensile cracks propagation is inhibited for confinement levels larger than about $1/10\sigma_1$ (Hoek and Bienawski, 1965). It is also justified by the fact that tensile stress conditions created by sample heterogeneities decreases with increasing confinement. In the term heterogeneities we include, following Lan et al. (2010), three different aspects: geometric heterogeneity which results from shape and size of grains, stiffness contrast of different grains, and contact heterogeneity due to grain contact length, orientation and stiffness anisotropy. If about 50% of the sample is under tensile conditions when uniaxially loaded (see Fig. 2), only a negligible part of the sample is under tension when confinement is larger than 1/10 of the *UCS* (18 MPa confinement in the case presented in Fig. 2). In these conditions, the initiation of tensile crack does occur, as tensile conditions at the tip of flaws still exist, but their propagation is prevented.

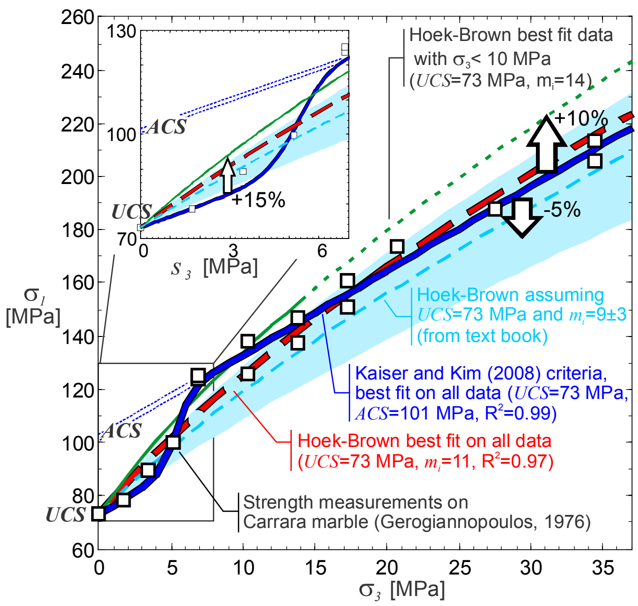


Figure 1. Laboratory test results of ultimate strength of Carrara marble under various confinements from Gerogiannopoulos, 1976) and various failure envelopes (see text for details).

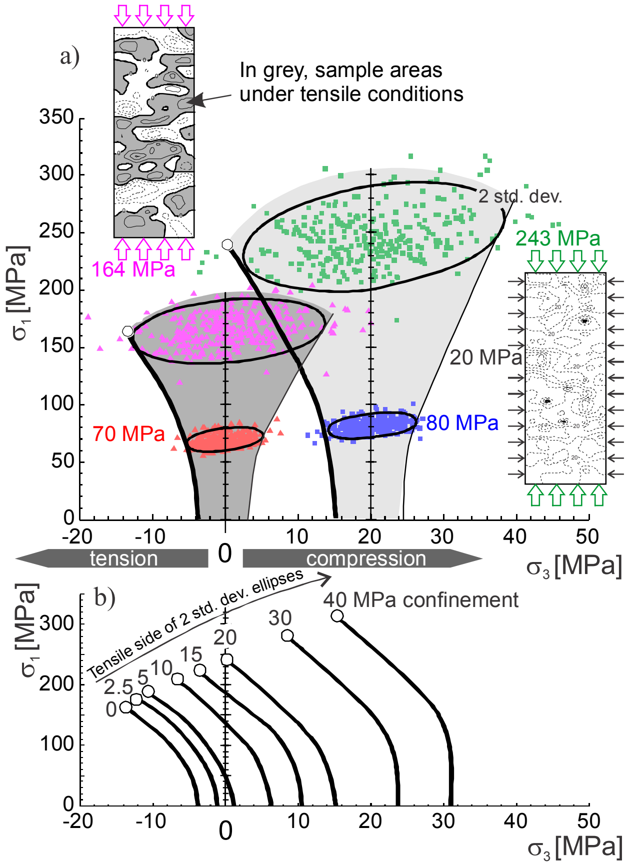


Figure 2: Illustration of the effect of heterogeneities on sample stress from PFC modeling after Diederichs (1999). *UCS* of the sample is 180 MPa:

a) Internal sample stress: red and magenta triangle, for zero confinement and with axial load of 70 MPa and 164 MPa, respectively. Blue and green squares: stress in a sample with 20 MPa confinement and 80 MPa and 243 MPa axial load, respectively. Black ellipses represent 2 standard deviation for a bivariate normal distribution (~95% confidence). Thick black lines represent the 2 standard deviation envelope on the tensile side. Inserts are $\sigma_3$ contours within the sample: areas shaded in grey are in tension.

b) Envelopes of 2 standard deviations on tensile side for confinement from 0 to 40 MPa. At low confinement level, significant area of the sample is under tensile conditions due to the presence of heterogeneities. At a confinement level larger than about 1/10 of *UCS*, sample areas in tension are negligible, preventing the unstable propagation of tensile cracks.

The Apparent Compressive Strength (*ACS*), conceptually similar to the apparent cohesion in Patton's joint failure theory (Patton, 1966), is obtained by projecting back to zero confinement a linear best fitted line through data at high confinement ($\sigma_3$>0.1*UCS*). For the data set presented on Fig. 1, *ACS* is equal to 101 MPa, i.e. 1.4*UCS*. Kim and Kaiser (2009) investigated the ratio of *ACS*/*UCS* by fitting sigmoidal failure criteria to laboratory testing data of 54 different rock types. It is found that almost all rock types in this set, from sedimentary rocks (coal, limestone, etc) to igneous and metamorphic rocks (granites, etc.), show some degree of brittleness. Moreover, it is found that the *ACS* is between 1 and 3 times the *UCS* or on average about 1.6 times higher than the *UCS*.

However, in terms of the quality of fit to the data the sigmoid criteria does not represent a statistically better fit as compared to the Hoek-Brown failure envelope. The coefficient of determination ($R^2$) is not significantly different for both fits on Fig. 1, being 0.97 for the Hoek-Brown envelope (red dashed curve on Fig. 1) and 0.99 the sigmoid envelope (blue curve on Fig. 1). This is typical for almost all data sets processed to date. That said, the primary objective of the sigmoid criteria is to create awareness of the broadly observed change of failure mechanism with increasing confinement and its importance for design purposes. It has also significant practical implications when determining the failure envelope of intact rock from data sets with incomplete confinement range. The next section deals with these practical implications.

## 2.2 *Interpretation of confinement limited data*

Frequently, triaxial testing is completed with only a few specimens and with confinements over an insufficient range, particularly for hard rocks where it is difficult to reach the recommended confinement range of $\geq 0.5$ *UCS* as stated in Hoek and Brown (1997) . This often results in data that is incorrectly processed and thus potentially misleading for design if the change in the failure mechanism with confinement is ignored.

Not every rock type should be expected to display changes in envelope curvature as shown in Fig. 1, but, at the very least, three transition zones should be considered when determining the confinements to be used in the testing and in the processing of data. These are: (1) $\sigma_3 < 0.1$ *UCS* – transition from long axial, relatively unsuppressed, tensile crack propagation to failure where tensile damage dominates but long axial cracks are suppressed by the confinement; (2) $\sigma_3 >$ *UCS* but $\sigma_1/\sigma_3 > 3.4$ – influence of confinement leading to shear band formation and thus predominantly shear failure processes with post-peak strength loss; and (3) $\sigma_1/\sigma_3 < 3.4$ (beyond Mogi's line) – the transition from stain-softening to ductile failure. Bewick et al. (2011) discuss these zones and the failure processes that dominate for different rock types at different confining stress levels in more detail.

The first two zones are shown on Fig. 1 and have practical implications. When a Hoek-Brown envelope is fitted to a limited data set with confinement <0.1 *UCS* (green line Fig. 1), the $m_i$-value and thus the strength at high confinement is overestimated by about 10%. At low confinement (1 to 6 MPa), the strength is overestimated by as much as ~15%. If only UCS data is available, and $m_i$ value is estimated from standard tables, e.g., for marble $m_i \sim 9\pm3$, the confined strength would be systematically underestimated (Fig. 1, cyan line with shaded range).

A practical approach to deal with these issues is to separate engineering problems in to inner and outer shell problems. In the inner shell, failure is dominated by spalling, tensile damage and potentially strain bursting. In the outer shell rock failure under sufficient confinement will be dominated by shear rupture and propagation. This approach will be presented in the next sections.

# 3 STRENGTH OF ROCK MASSES

The strength of rock masses is typically estimated by coupling characteristic rock mass descriptors with empirical relationships, e.g., the Geological Strength Index *GSI,* and the generalized Hoek-Brown empirical failure criterion (Hoek et al., 2002). In this approach, the intact rock strength is degraded to some lower value to take into account the effects of block size and fractures that reduce both the cohesion and frictional properties. The degradation factors have been evaluated empirically and are valid for the range of conditions covered by the supporting experience. The approach underlying the calibration of the *GSI*/generalized Hoek-Brown relationship mostly stems from experience gained by back-analyses of tunnels (Hoek et al., 1995). Hence, it must be assumed that the back-analyzed parameters are most representative for the low confinement range (inner shell behavior).

Conceptually the system is designed for rock masses for which block size and incipient strength are such that rock mass behavior tends to be controlled by inter-block shear strength rather than the intact rock strength (Carter et al., 2008). According to these authors, for rock mass with very low intact rock strength (*UCS*<15 MPa) and for hard brittle rock masses (*GSI*>65, $m_i$>15), strength estimation from the generalized Hoek-Brown relations and GSI are not recommended. At high confinement, it is to be expected that rough joints will be strongly interlocked and failure through intact rock (shearing of asperities or coalescence through rock bridge failure) will be controlling the strength of the rock mass. If this were the case, then degradation factors back-analyzed from inner shell behavior should underestimate the rock mass strength in the outer shell. The question thus is how much the degradation factors change with increasing confinement.

Measuring reliably rock mass strength under confined conditions in situ is difficult if not impossible and to our knowledge no such data with sufficient quality and quantity exists. For this reason and to illustrate the proposed confinement dependent degradation concept, we present on Fig. 3 data from a suite of laboratory tests on a quartzite. This quartzite is affected by numerous micro-defects with variable intensity and thus is thought to represent an analog for a rock mass, with higher micro-defect intensity corresponding to lower rock mass competency (e.g. lower *GSI*).

In Fig. 3, the upper end of the test results can be fitted with a Hoek-Brown (*UCS* = 245 MPa, $m_i$ = 26) or a sigmoid function (*UCS* = 245 MPa, *ACS* = 320 MPa) and is assumed to correspond to the intact rock strength (*GSI* = 100). The generalized Hoek-Brown strength envelopes (Hoek and Brown, 1997) for *GSI* = 80, 60 and 50 are also displayed in gray on Fig. 3; i.e., under confined conditions ($\sigma_3$>0.1*UCS*) the strength reduction is assumed to follow the same degradation amount than for the low confinement domain. For <~0.05*UCS*, the strength reduction with decreasing *GSI* is consistent with the increasing influence of micro-defects (see failure type shown in Fig. 3). However, the corresponding strength for high confinement (> 0.06*UCS*) is not in agreement with the test data that shows little variability and strength reduction (we recognize that the number of data points is rather limited in this range).

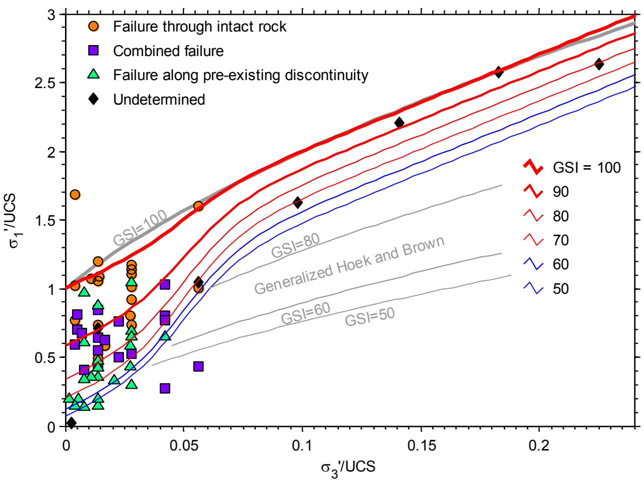


Figure 3: Sigmoid failure envelope for rock masses with hypothetical reduced degradation under high confinement overlain on laboratory strength data of quartzite with variable intensity of micro-defects and confinement.

In order to better reflect the data trend with increasing confinement, we used the sigmoid function and applied different degradation factors to *UCS* and *ACS*. The degradation logic follows the generalized Hoek-Brown approach with $UCS_{\text{rockmass}} = UCS{\cdot}s^{a}$ . The variables $s$ and $a$ are functions of *GSI* and their formulation as given in (Hoek et al., 2002) are used to degrade *UCS*. However, for *ACS* the constant in the denominator of the formulation of $s$ which is set to the value of $C_s$=9 in Hoek et al. (2002) is altered and for the example shown is set at $C_s$=50 in order to reduce the degradation under confinement as presented on Fig. 3. It is obvious that the amount and quality of data presented on Fig. 3 does not allow one to ascertain the appropriate degradation factor but it clearly suggests that the degradation factor ($C_s$) for confined rock may be an order of magnitude larger. This aspect is the focus of further research, but we suggest that the discrepancy between the actual confined strength of rock masses and the strength obtain by using the generalized Hoek-Brown approach could be as significant as presented on Fig. 3.

In view of these results it is suggested that the rock mass strength and behavior may differ significantly in the direct vicinity of openings or in the inner shell and remote from excavations, i.e. in the outer shell. For these reasons, it is recommended to use for design a differentiated approach to obtain the failure envelope and to assess potential failure modes in the inner or the outer shell. Such differentiated approaches are discussed in the following sections.

### 3.1 *Inner shell problems: tensile failure leading to spalling*

In the inner shell, under low confinement, the failure mode will be dominated by tensile cracking leading to spalling and related geometric dilation processes. A number of field studies have shown that for brittle rocks, spalling initiates at tangential stress levels significantly below the *UCS*, even for rock masses with virtually no joints (*GSI*=100). In situ strengths as low as 0.4*UCS* were back-analyzed, although such estimates must rely on independent stresses estimates at the location of spalling, which are rarely highly reliable. Probably the best constrained case reported to date is by Anderson and Martin (2009) at the Aspö laboratory as part of the stress leading to spalling was thermally induced and therefore somewhat controlled. A spalling strength of 0.59*UCS* was back-calculated in this case. The reason for such a difference in strength between laboratory and in situ measurements still remains uncertain as in both cases the same mechanism, unstable tensile crack propagation, leads to final failure. Proposed explanations include differences in stress path, stress rotations, geometrical effects and loading system stiffness, but none of these potential effects have been fully verified.

Furthermore, not all rock masses are affected to the same degree by the spalling process. Carter et al. (2009) proposed an approach to identify intermediate cases based on the ratio $UCS\,/\,\sigma_T$. Their proposed deviation from *GSI*/Hoek-Brown degradation scheme at $\sigma_3 = 0$ is presented on Fig. 4A. According to their relation, for $UCS\,/\,\sigma_T$<11 *GSI* applies. For $UCS\,/\,\sigma_T$>17 , the unconfined rock mass strength reduces to about 0.4*UCS*. In practice, application of their criteria based on $UCS\,/\,\sigma_T$ is delicate because it is very sensitive to the estimation of the tensile strength. A change of $\sigma_T$ of only 20% (e.g. from 8.3 to 6.7) induces a change of rock mass strength of 40% (assuming UCS=100 MPa). Also some significant discrepancies from their relation can be observed (e.g. URL granodiorite, Fig. 4B).

Alternate approaches to determine the failure parameters of brittle rocks were proposed by Diederichs et al. (2004) and Suorineni et al. (2009). Both studies proposed empirical rating systems to evaluate the spalling strength of rocks. They are motivated by the following observation, which was made the at Underground Rock Laboratory (URL) in Manitoba: Tunnel sections passing through granodiorite and granite with very similar mineralogical composition (actually, despite their misleading names, both are granite according to QAPF classification) and similar $UCS/\sigma_T$ ratio, but different grain size distribution (the granite with a coarser and more broadly distributed grain size) performed

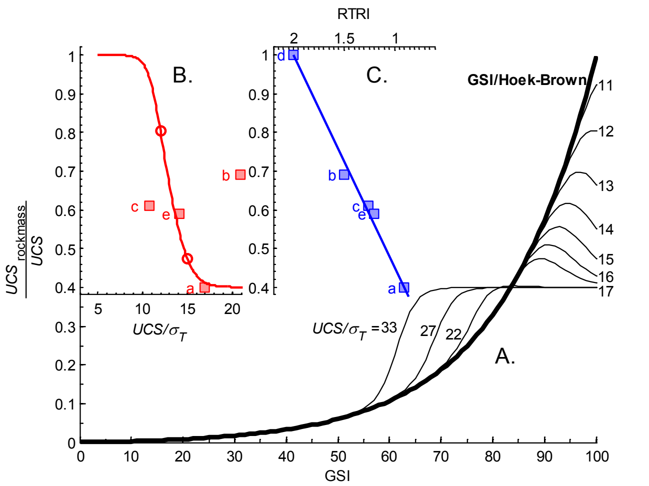


Figure 4: A. Modification of the *GSI*/Hoek-Brown approach for spalling rocks after Carter et al. (2009); B. degradation of unconfined rock mass strength at *GSI*=100 as a function of the ratio of $UCS\,/\,\sigma_T$ according to Carter et al. relation; C. degradation of unconfined rock mass strength following the approach developed in Suorineni et al. (2009). Data point on B. and C.: a, b. URL granite and granodiorite (Martin et al. 1999). c. Thompson Quartzite (Suorineni et al., 2009). d. hypothetical uni-mineral rock (Suorineni et al., 2009). e. Aspö diorite (Johansson, 1998; Andersson et al., 2009).

differently in the same stress conditions. A depth of failure of about 30% of tunnel radius was observed for the URL granite, while the granodiorite showed a depth of failure of zero at the same stress level. This finding has obvious implications for support selection and drift advance, as it drastically changes the support requirements. Whereas it is shown that texture plays a very important role in rock mass tenacity to stress-induced damage, several components of texture are not yet accounted for in the Rock Tenacity Rating Index (RTRI) system (Suorineni et al., 2009) and more field cases are required to validate the system (Fig. 4C).

In order to further assess the failure of brittle rock in the direct vicinity of excavations, the unconfined compressive rock mass strength describe above must be complemented by the spalling limit as described in Martin et al. (1999), Kaiser et al. (2000) and its practical application for modeling by Diederichs et al. (2007). The spalling limit operates the transition from the unconfined condition to the confined conditions, the focus of the next section.

### 3.2 *Outer shell problems: crack damage leading to shear failure*

The strength difference between the generalized Hoek-Brown/*GSI* approach and the sigmoid envelope with hypothetical degradation factor under confinement presented on Fig. 3 becomes particularly relevant for confined rock mass problems such as those encountered in the core of relatively wide pillars (Kaiser et al., 2010). For such cases, the strength of pillar core is potentially much higher than would be estimated by the Hoek-Brown relation. An evaluation of the impact of this hypothesis on pillar strength is developed in Kaiser et al. (2010) and presented on Fig. 5. For narrow pillars with low $W/H$ ratios, failure is dominated by spalling and both criteria lead to similar results. However, for intermediate to large $W/H$ ratios, the differences between the two approaches are significant. Such elevated strength of pillar cores is supported by data in the pillar failure databases (see Kaiser et al., 2010 for details). Few if any pillar failures are reported for $W/H > 2$ and this is consistent with experiences with wide pillars in South African mines.

The consequences for pillar design are two-folded: 1) pillar design can possibly be optimized, using smaller $W/H$ ratios and still insuring the carrying capacity of the pillar, and 2) pillars that would be assumed to be in the yielding state based on the Hoek-Brown/*GSI* failure envelope could have a core that actually is in pre-peak conditions, i.e. still accumulating stress and potentially entering into a burst prone state.

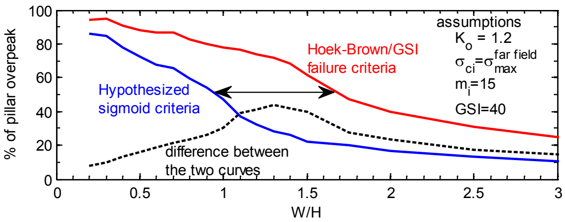


Figure 5: Comparison of failure severity of pillar with various $W/H$ ratios assuming the Hoek-Brown (red) or the hypothesized sigmoidal failure criteria (blue) (see Kaiser et al., 2010). This figure indicates that the difference between the two approaches is greatest at $1 < W/H < 2$.

## 4 CONCLUSIONS

The change of failure mode of rock and rock masses with increasing confinement has been recognized for a long time, but assessing its impact on the strength of intact rock and particularly of rock masses is not embedded in commonly used failure criteria (Mohr-Coulomb or Hoek-Brown). In order to remediate this situation, we propose to differentiate the approach for strength determination when solving problems affected by low confinement, which we refer to as inner shell problems, and problems controlled by high confinement or outer shell problems (Fig. 6).

Numerous publications deal with the inner shell problem and related spalling processes. It has been shown that under these conditions, rock strength reduces significantly and the rock mass tends to bulk as it is being deformed. Practical approaches (Martin et al., 1999; Kaiser et al., 2001; Diederichs et al., 2004; Carter et al., 2009; Suorineni et al., 2009) have been proposed to evaluate the spalling strength and its impact on inner shell behavior.

The strength of highly confined, massive to moderately jointed, hard rock masses in the outer shell remains largely an open question, but we suggest that it is significantly higher than estimated by the Hoek-Brown/*GSI* approach. Its quantification is the focus of current research. For now we tentatively propose the use of a degradation constant of $C_s = 50$ for the highly confined range of the Hoek-Brown relationships. This recommendation however needs to be verified by systematic back-analyses.

A corollary of the recognition that strength in the inner shell and outer shell significantly differs is that special care must be taken when calibrating numerical models. Particularly, one must ensure that the calibration process covers the full confinement range of the problem at hand. Calibrating models on inner shell problems (e.g. opening wall failure and related seismicity) alone and applying the resulting parameters for outer shell problems (e.g. pillar design) may result in designs that are either over-conservative (with premature yield) or risky (with unexpected burst proneness).

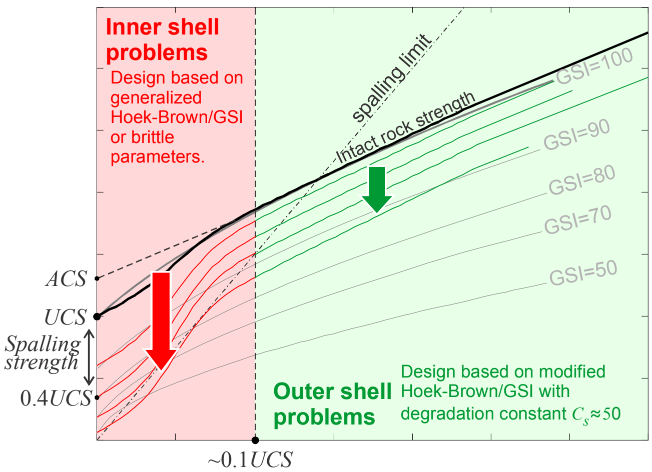


Figure 6: Proposed approach to differentiate failure envelope for inner shell and outer shell problems.

## 5 AKNOWLEDGMENTS

This research is supported by CEMI's industrial sponsors, the Government of Ontario through its Ministry of Research and Innovation and by NSERC (Natural Sciences and Engineering Research Council of Canada).

*REFERENCES*

Andersson, J. C., Martin, C. D., Stille, H., 2009. The Äspö Pillar Stability Experiment: Part II–Rock mass response to coupled excavation-induced and thermal-induced stresses. *Int. J. Rock Mech. Min. Sc.* 46 (5): 879–895.

Bewick, R.P.. Kaiser, P.K., and Bawden, W.F. (2011 – to be submitted). Understanding triaxial testing data and practical implications for the estimation of the mi value. *To be submitted to the American Rock Mechanics Symp.*, San Francisco, 2011.

Carter, T. G., Diederichs, M. S., Carvalho, J. L., 2008. Application of modified Hoek-Brown transition relationships for assessing strength and post yield behaviour at both ends of the rock competence scale. *J. South. Afr. Inst. of Min. and Met.* 108: 325–338.

Diederichs, M. S., 2003. Manuel Rocha Medal Recipient Rock Fracture and Collapse Under Low Confinement Conditions. *Rock Mech. Rock Eng.* 36 (5): 339–381.

Diederichs, M. S., Kaiser, P. K., Eberhardt, E., 2004. Damage initiation and propagation in hard rock during tunnelling and the influence of near-face stress rotation *Int. J. Rock Mech. Min. Sc.* 41 (5): 785-812.

Gerogiannopoulos, N. G., 1976. A Critical State Approach to Rock Mechanics. Ph.D. thesis, University of London.

Gramberg, J., 1989. A Non-Conventional View on Rock Mechanics and Fracture Mechanics. A.A. Balkema, Rotterdam, Nertherlands.

Griffith, A. A., 1920. The phenomena of rupture and flow in solids. *Philos. T. Roy. Soc. A*, 221: 163–198.

Hoek, E., Bieniawski, Z. T., 1965. Brittle rock fracture propagation in Rock under compression. *Int. J. Fract. Mech.* 1 (3): 137–155.

Hoek, E., Kaiser, P. K., Bawden, W. F., 1995. Support of Underground Excavations in Hard Rock. Taylor & Francis.

Hoek, E., Brown, E. T., 1997. Practical estimates of rock mass strength. *Int. J. Rock Mech. Min. Sc.* 34(8): 1165–1186.

Hoek, E., Carranza-Torres, C. T., Corkum, B. T., 2002b. Hoek-Brown failure criterion. In: Hammah, Bawden, Curran, Telesmicki (Eds.), *Proc. of the 5th North Amer. Rock Mechanics Symposium*. University of Toronto: 267–274.

Johansson, H., 1998. Diffusion pathways in crystalline rock - examples from Äspö-diorite and fine-grained granite. *J. Contam. Hydrol.* 35 (1-3): 41–53.

Kaiser, P. K., Diederichs, M. S., Martin, C. D., Sharp, J., Steiner, W., November 2001. Underground works in hard rock tunneling and mining. In: Geo-Eng2000. *Int. Conf. Geotech. and Geol. Eng.* 1: 841-926.

Kaiser, P. K., Kim, B. H., 2008. Rock mechanics advances for underground construction in civil engineering and mining. In: *Korean Symposium of Rock Mechanics.* Seoul.

Kemeny, J. M. and Cook, N. W. G. 1987. Crack models for the failure of rocks in compression. *In: Constitutive Laws for engineering material: Theory and applications*, Desai et al. (eds). Elsevier, Amsterdam, 2: 879–887.

Kaiser, P. K., Kim, B.-H., Bewick, R. P., Valley, B., 2010. Rock mass strength at depth and implications for pillar design. In: *Deep Mining 2010 - 5th international seminar on deep and high stress mining*, Van Sint Jan, M and Potvin, Y. (eds.), Santiago, Chile. Australian Center for Geomechanics: 463–476.

Kim, B. H. and Kaiser, P. K., 2009. Rock strength characterization for excavations in brittle failing rocks. In: *ROCKENG09: Proc. of the 3rd CANUS Rock Mech. Symp.* Diederichs, M., Grasselli, G. (eds.). Toronto.

Lan, H., Martin, C. D., Hu, B., 2010. Effect of heterogeneity of brittle rock on micromechanical extensile behavior during compression loading. *J. Geophys. Res.*, 115, B01202: 14p.

Martin, C. D., Kaiser, P. K., McCreath, D., 1999. Hoek-Brown parameters for predicting the depth of brittle failure around tunnels. *Can. Geotech. J.* 36: 136–151.

Patton, F. D., 1966. Multiple mode of shear failure in rock. In: *1st International Conference of Rock Mechanics*. Lisbon: 509–513.

Steiner, W., Kaiser, P. K., Spaun, G., 2010. Role of brittle fracture on swelling behaviour of weak rock tunnels: hypothesis and qualitative evidence *Geomechanik Tunnelbau* 3 (5): 583-596.

Suorineni, F. T., Chinnasane, D., Kaiser, P. K., December 2009. A Procedure for Determining Rock-Type Specific Hoek-Brown Brittle Parameter s. *Rock Mech. Rock Eng.* 42 (6): 849-881.

Valley, B., Suorineni, F. T., Kaiser, P. K., 2010. Numerical analyses of the effect of heterogeneities on rock failure process. In: *44th U.S. Rock Mechanics Symposium and 5th U.S.-Canada Symposium*. Salt Lake City. ARMA 10–648.